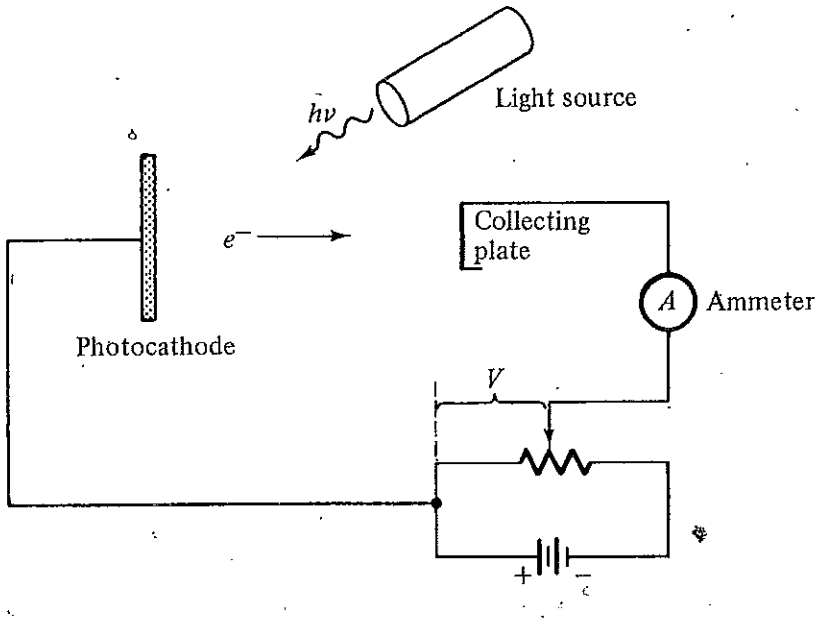

FIGURE 2.3 Photoelectric experiment.

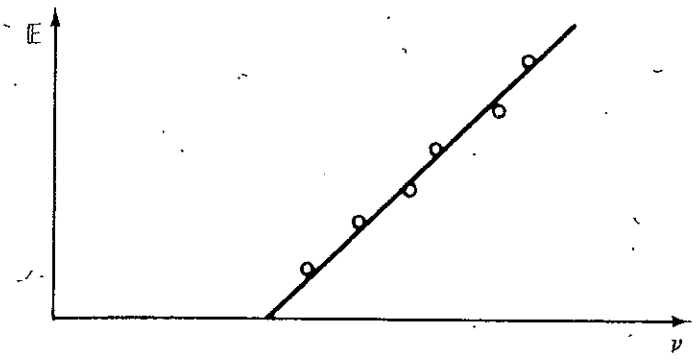

FIGURE 2.4 Typical data showing energy of most energetic electrons as a function of frequency ν in the photoelectric experiment.

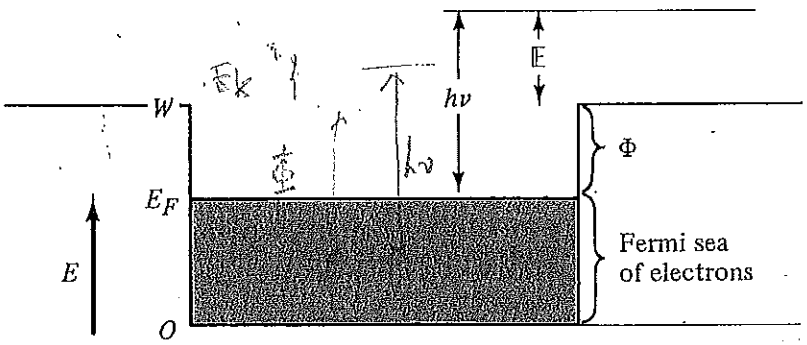

FIGURE 2.5 Sommerfeld model for energy distribution of electrons in a metal.

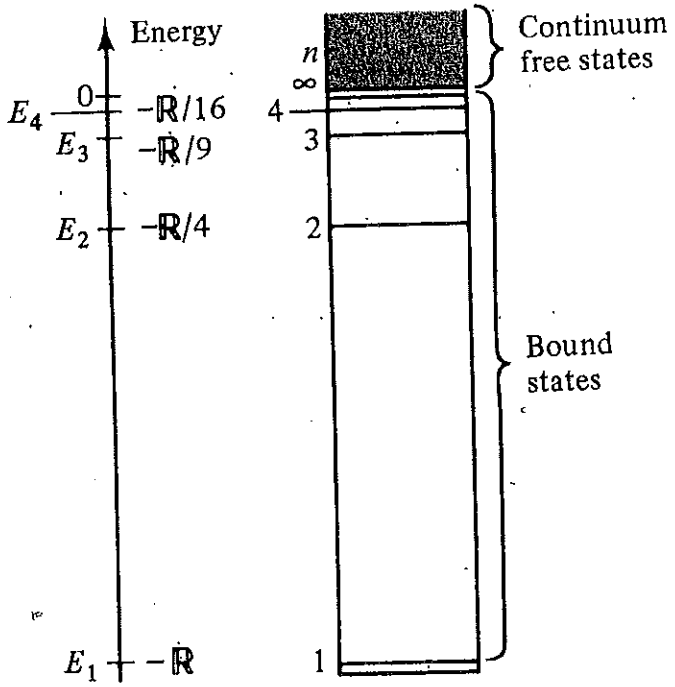

FIGURE 2.7 Bohr spectrum.

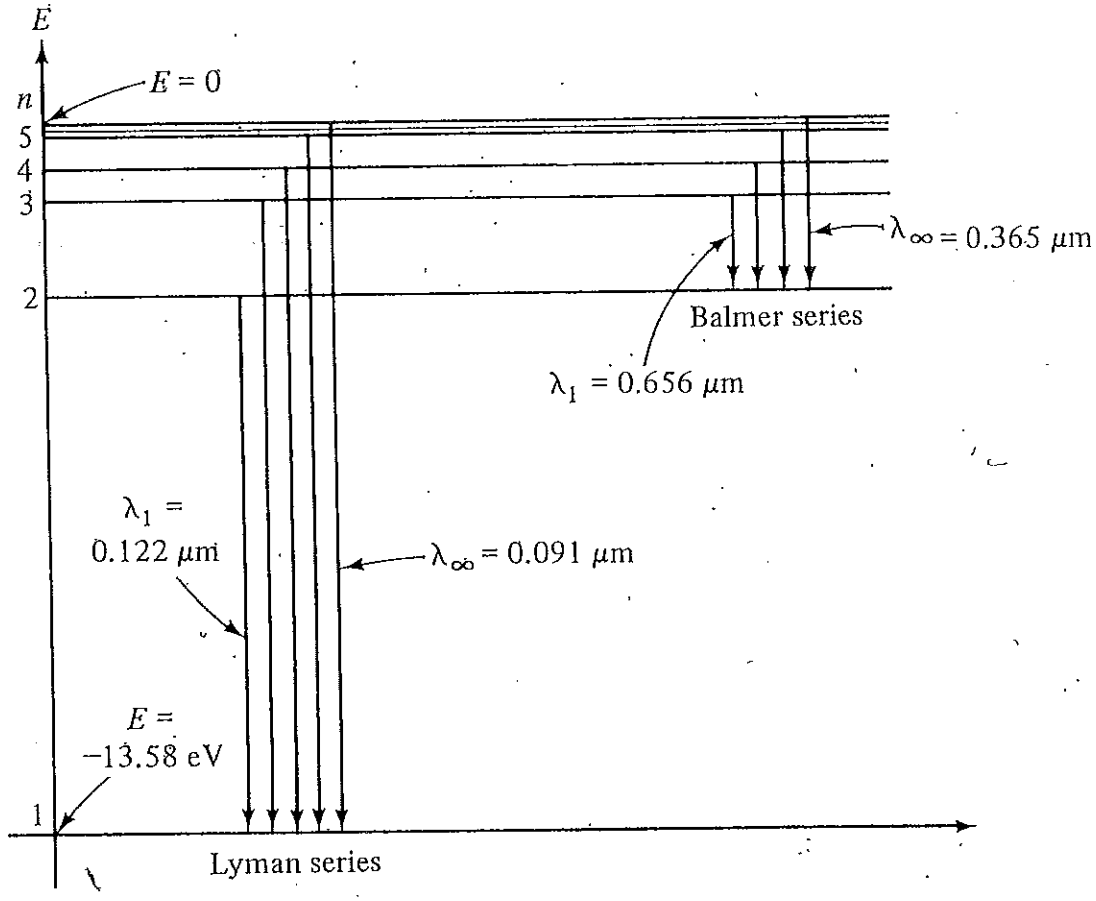

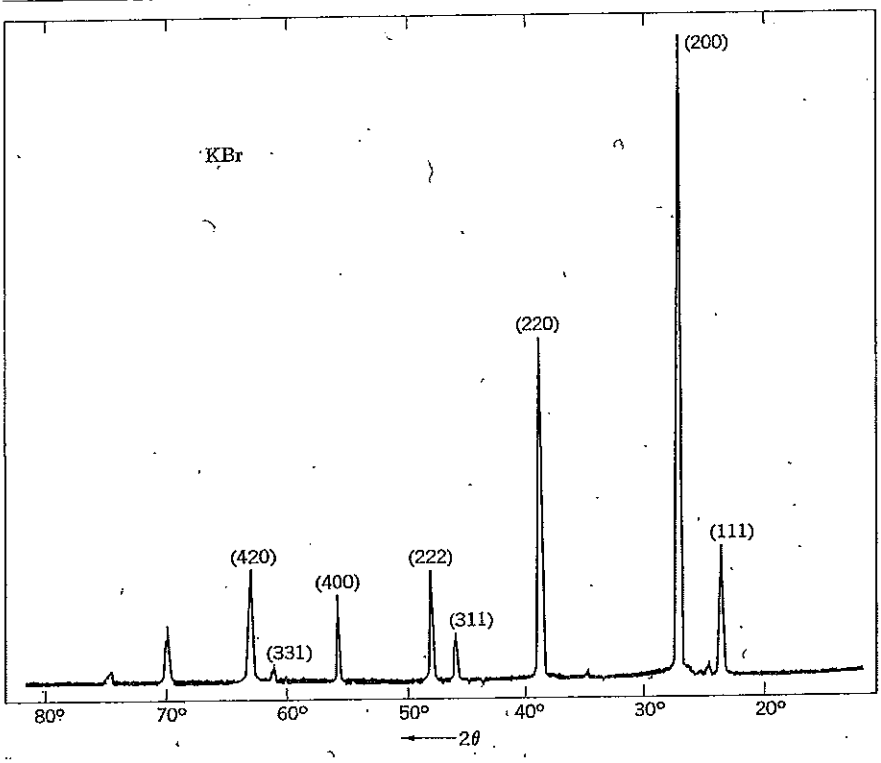

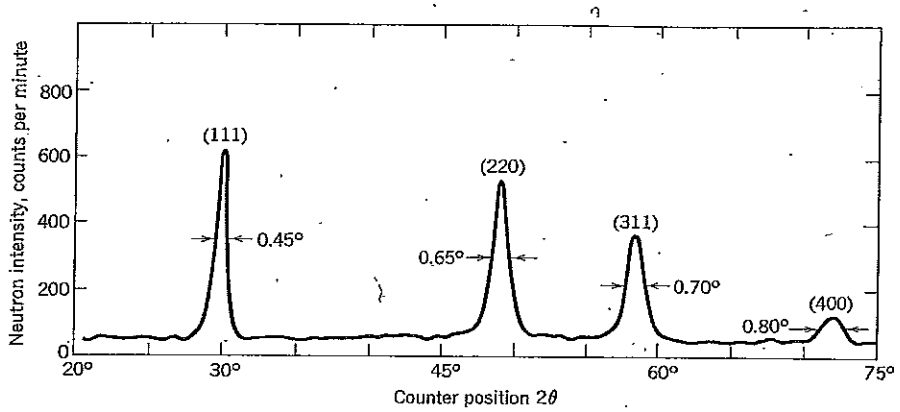

Figure 30 Neutron diffraction pattern for powdered diamond. (After G. Bacon.)

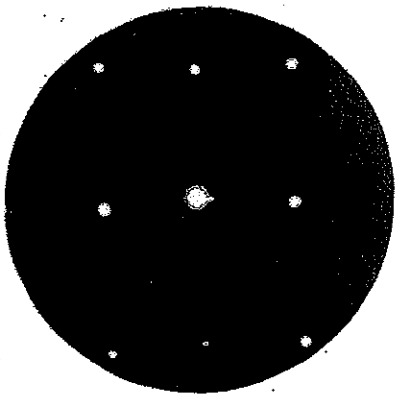

(a)

Figure 29 (a) Backward scatterin mally on the (110) face of a nickel (b). (Courtesy of A. U. MacRae.)

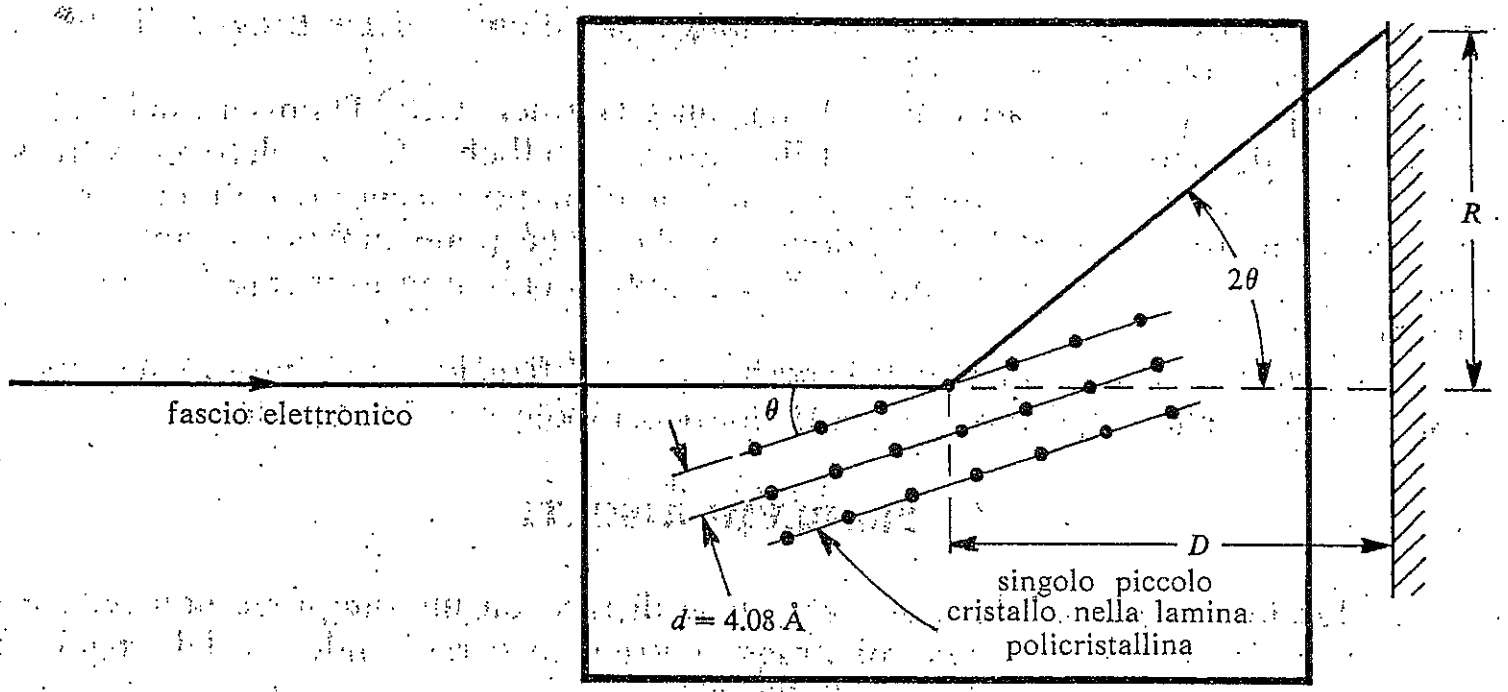

Fig. 16-3

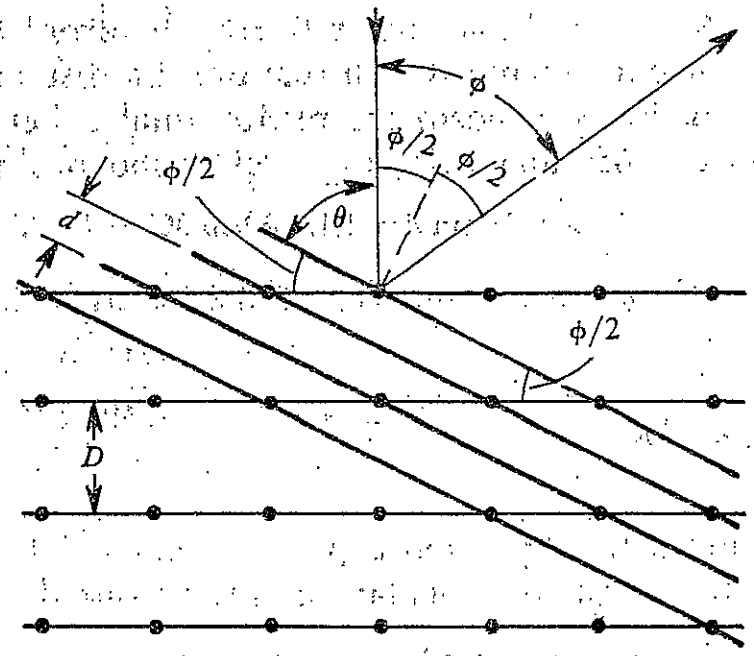

Fig. 16-5

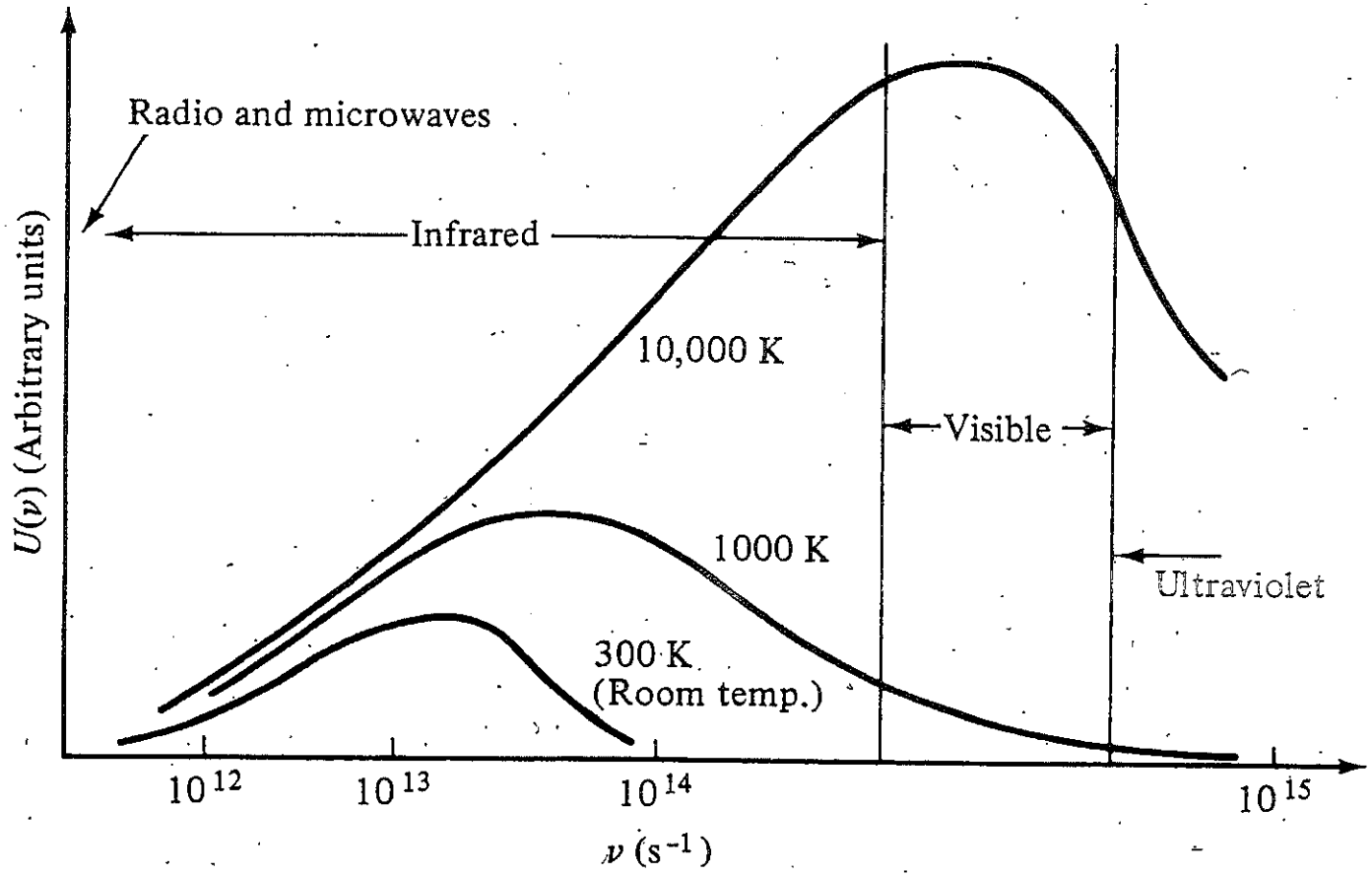
Radio and microwaves
Infrared
10,000 K
Visible
1000 K
Ultraviolet
300 K
(Room temp.)
$U(\nu)$ (Arbitrary units)
10^{12}
10^{13}
10^{14}
10^{15}
ν (s^{-1})

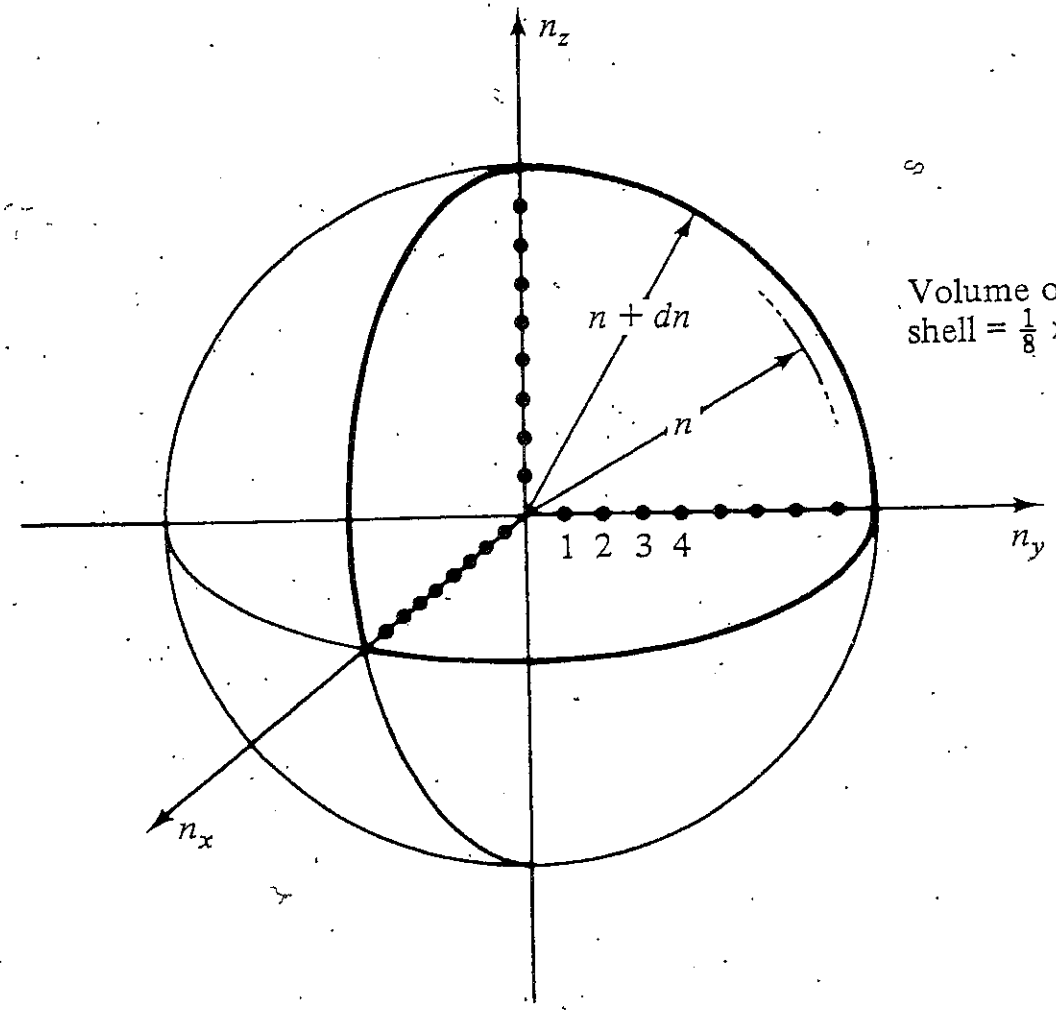

Volume of spherical shell = $\frac{1}{8} \times 4\pi n^2\, dn$

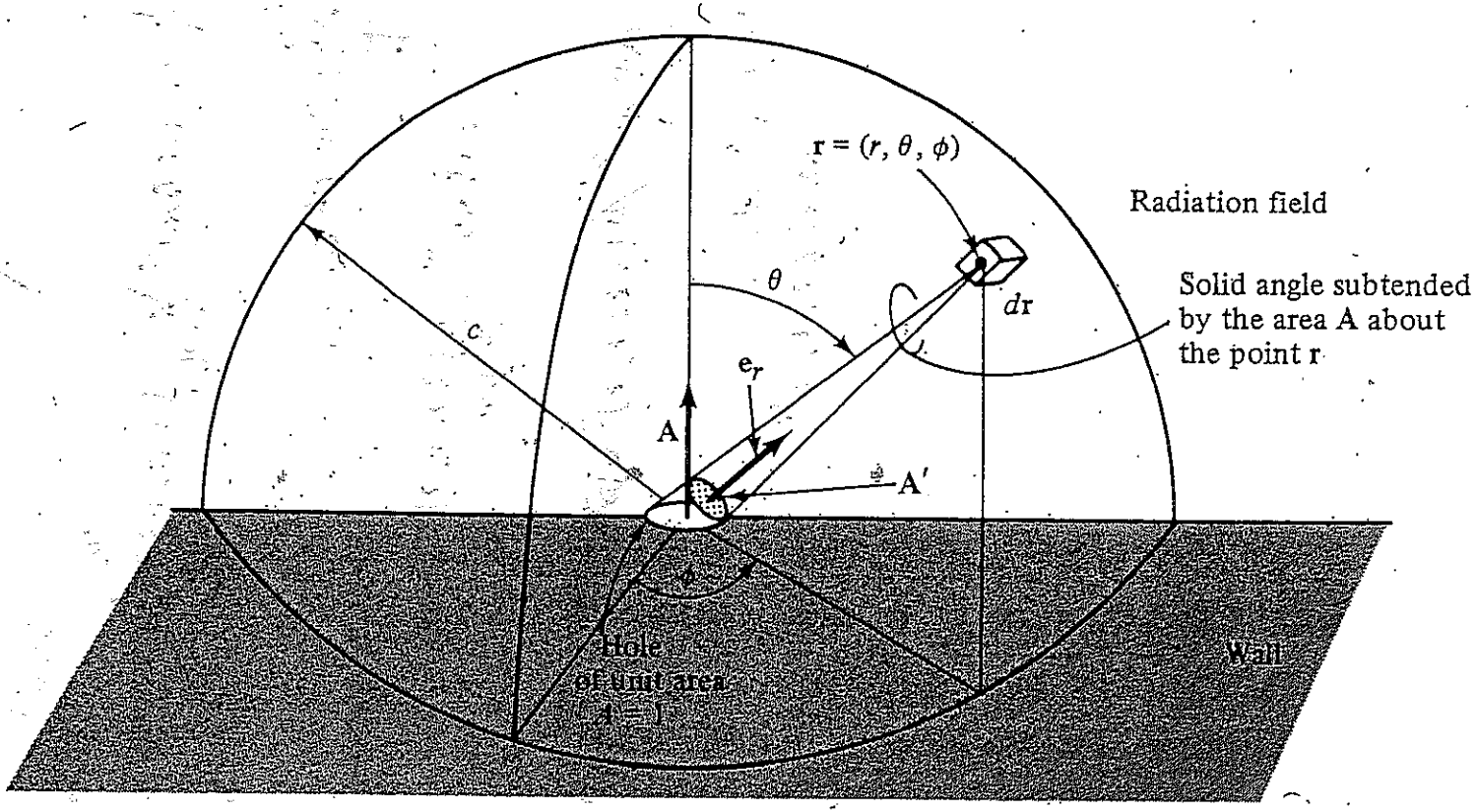
r = (r, θ, φ)
Radiation field
Solid angle subtended by the area A about the point r
dr
θ
c
e_r
A
A′
Hole of unit area
Wall

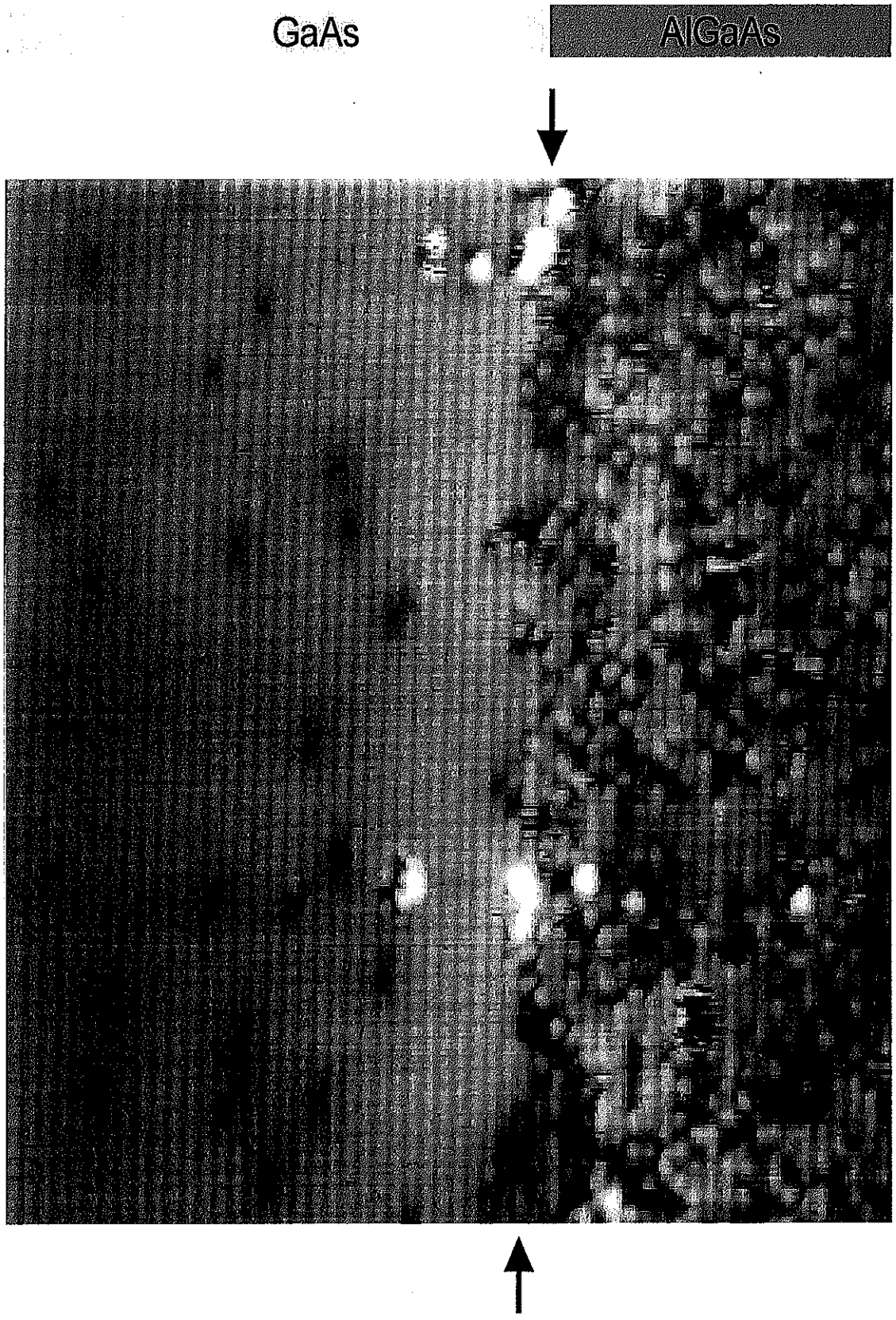
GaAs
AlGaAs

DRUDE RELAXATION TIMES IN UNITS OF 10^{-14} SECOND[a]

ELEMENT	77 K	273 K	373 K
Li	7.3	0.88	0.61
Na	17	3.2	
K	18	4.1	
Rb	14	2.8	
Cs	8.6	2.1	
Cu	21	2.7	1.9
Ag	20	4.0	2.8
Au	12	3.0	2.1
Be		0.51	0.27
Mg	6.7	1.1	0.74
Ca		2.2	1.5
Sr	1.4	0.44	
Ba	0.66	0.19	
Nb	2.1	0.42	0.33
Fe	3.2	0.24	0.14
Zn	2.4	0.49	0.34
Cd	2.4	0.56	
Hg	0.71		
Al	6.5	0.80	0.55
Ga	0.84	0.17	
In	1.7	0.38	0.25
Tl	0.91	0.22	0.15
Sn	1.1	0.23	0.15
Pb	0.57	0.14	0.099
Bi	0.072	0.023	0.016
Sb	0.27	0.055	0.036

[a] Relaxation times are calculated from the data in Tables 1.1 and 1.2, and Eq. (1.8). The slight temperature dependence of n is ignored.

Figure 9 Experimental heat capacity values for potassium, plotted as C/T versus T^2. (After W. H. Lien and N. E. Phillips.)

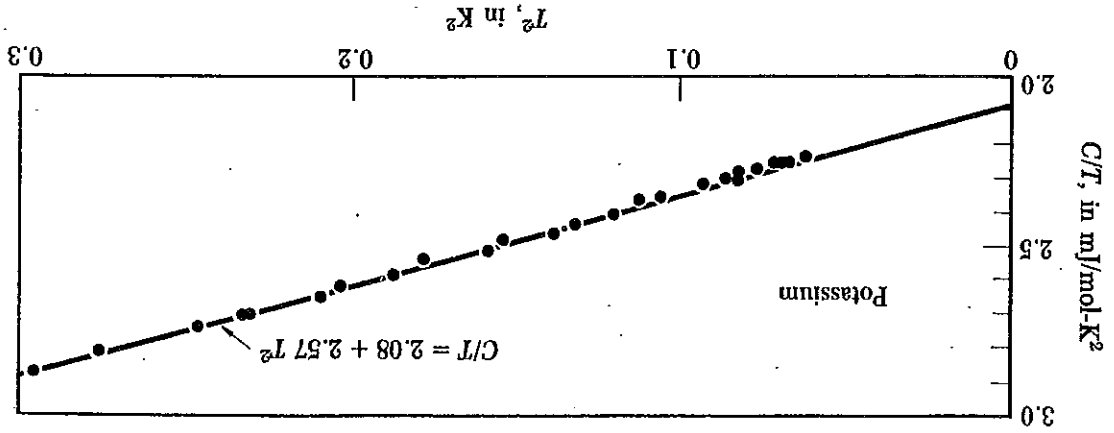

Table 2.2
BULK MODULI IN 10^{10} DYNES/CM^2 FOR SOME TYPICAL METALS[a]

METAL	FREE ELECTRON B	MEASURED B
Li	23.9	11.5
Na	9.23	6.42
K	3.19	2.81
Rb	2.28	1.92
Cs	1.54	1.43
Cu	63.8	134.3
Ag	34.5	99.9
Al	228	76.0

[a] The free electron value is that for a free electron gas at the observed density of the metal, as calculated from Eq. (2.37).

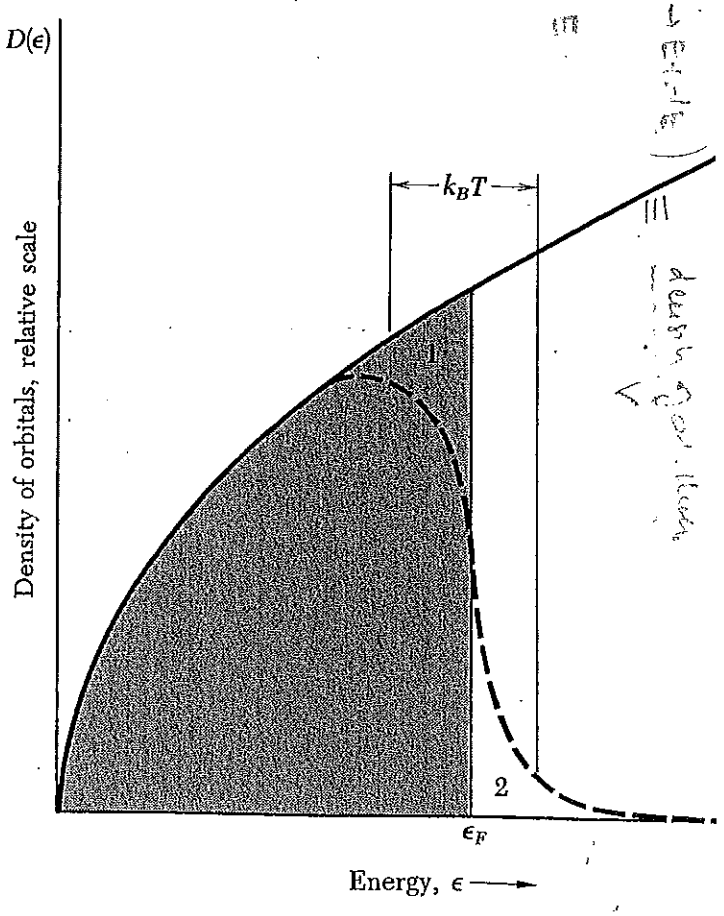

Figure 5 Density of single-particle states as a function of energy, for a free electron gas in three dimensions. The dashed curve represents the density $f(\epsilon,T)D(\epsilon)$ of filled orbitals at a finite temperature, but such that k_BT is small in comparison with ϵ_F. The shaded area represents the filled orbitals at absolute zero. The average energy is increased when the temperature is increased from 0 to T, for electrons are thermally excited from region 1 to region 2.

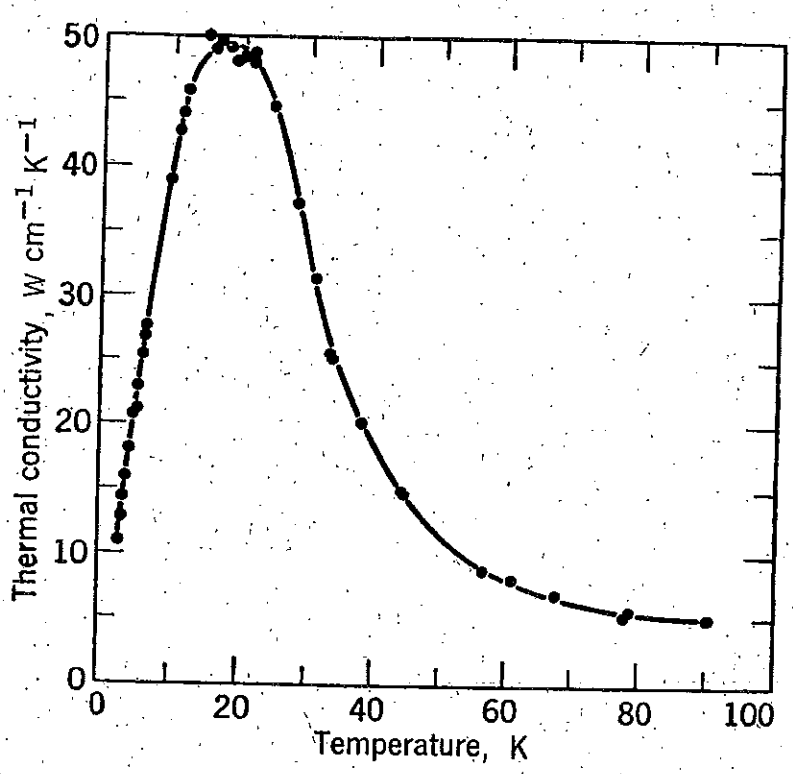

Figure 11 The thermal conductivity of copper, after Berman and MacDonald.

Table 1.6
EXPERIMENTAL THERMAL CONDUCTIVITIES AND LORENZ NUMBERS OF SELECTED METALS

ELEMENT	273 K		373 K	
	κ (watt/cm-K)	$\kappa/\sigma T$ (watt-ohm/K^2)	κ (watt/cm-K)	$\kappa/\sigma T$ (watt-ohm/K^2)
Li	0.71	2.22×10^{-8}	0.73	2.43×10^{-8}
Na	1.38	2.12		
K	1.0	2.23		
Rb	0.6	2.42		
Cu	3.85	2.20	3.82	2.29
Ag	4.18	2.31	4.17	2.38
Au	3.1	2.32	3.1	2.36
Be	2.3	2.36	1.7	2.42
Mg	1.5	2.14	1.5	2.25
Nb	0.52	2.90	0.54	2.78
Fe	0.80	2.61	0.73	2.88
Zn	1.13	2.28	1.1	2.30
Cd	1.0	2.49	1.0	
Al	2.38	2.14	2.30	2.19
In	0.88	2.58	0.80	2.60
Tl	0.5	2.75	0.45	2.75
Sn	0.64	2.48	0.60	2.54
Pb	0.38	2.64	0.35	2.53
Bi	0.09	3.53	0.08	3.35
Sb	0.18	2.57	0.17	2.69

Source: G. W. C. Kaye and T. H. Laby, *Table of Physical and Chemical Constants*, Longmans Green, London, 1966.

Table 4 Comparison of observed Hall coefficients with free electron theory

[The experimental values of R_H as obtained by conventional methods are summarized from data at room temperature presented in the Landolt-Bornstein tables. The values obtained by the helicon wave method at 4 K are by J. M. Goodman. The values of the carrier concentration n are from Table 1.4 except for Na, K, Al, In, where Goodman's values are used. To convert the value of R_H in CGS units to the value in volt-cm/amp-gauss, multiply by 9×10^{11}; to convert R_H in CGS to m^3/coulomb, multiply by 9×10^{13}.]

Metal	Method	Experimental R_H, in 10^{-24} CGS units	Assumed carriers per atom	Calculated $-1/nec$, in 10^{-24} CGS units
Li	conv.	−1.89	1 electron	−1.48
Na	helicon	−2.619	1 electron	−2.603
	conv.	−2.3		
K	helicon	−4.946	1 electron	−4.944
	conv.	−4.7		
Rb	conv.	−5.6	1 electron	−6.04
Cu	conv.	−0.6	1 electron	−0.82
Ag	conv.	−1.0	1 electron	−1.19
Au	conv.	−0.8	1 electron	−1.18
Be	conv.	+2.7	—	—
Mg	conv.	−0.92	—	—
Al	helicon	+1.136	1 hole	+1.135
In	helicon	+1.774	1 hole	+1.780
As	conv.	+50.	—	—
Sb	conv.	−22.	—	—
Bi	conv.	−6000.	—	—

Table 1 Calculated free electron Fermi surface parameters for metals at room temperature

(Except for Na, K, Rb, Cs at 5 K and Li at 78 K)

Valency	Metal	Electron concentration, in cm^{-3}	Radius[a] parameter r_s	Fermi wavevector, in cm^{-1}	Fermi velocity, in cm s^{-1}	Fermi energy, in eV	Fermi temperature $T_F \equiv \epsilon_F/k_B$, in deg K
1	Li	4.70×10^{22}	3.25	1.11×10^8	1.29×10^8	4.72	5.48×10^4
	Na	2.65	3.93	0.92	1.07	3.23	3.75
	K	1.40	4.86	0.75	0.86	2.12	2.46
	Rb	1.15	5.20	0.70	0.81	1.85	2.15
	Cs	0.91	5.63	0.64	0.75	1.58	1.83
	Cu	8.45	2.67	1.36	1.57	7.00	8.12
	Ag	5.85	3.02	1.20	1.39	5.48	6.36
	Au	5.90	3.01	1.20	1.39	5.51	6.39
2	Be	24.2	1.88	1.93	2.23	14.14	16.41
	Mg	8.60	2.65	1.37	1.58	7.13	8.27
	Ca	4.60	3.27	1.11	1.28	4.68	5.43
	Sr	3.56	3.56	1.02	1.18	3.95	4.58
	Ba	3.20	3.69	0.98	1.13	3.65	4.24
	Zn	13.10	2.31	1.57	1.82	9.39	10.90
	Cd	9.28	2.59	1.40	1.62	7.46	8.66
3	Al	18.06	2.07	1.75	2.02	11.63	13.49
	Ga	15.30	2.19	1.65	1.91	10.35	12.01
	In	11.49	2.41	1.50	1.74	8.60	9.98
4	Pb	13.20	2.30	1.57	1.82	9.37	10.87
	Sn(w)	14.48	2.23	1.62	1.88	10.03	11.64

[a]The dimensionless radius parameter is defined as $r_s = r_0/a_H$, where a_H is the first Bohr radius and r_0 is the radius of a sphere that contains one electron.

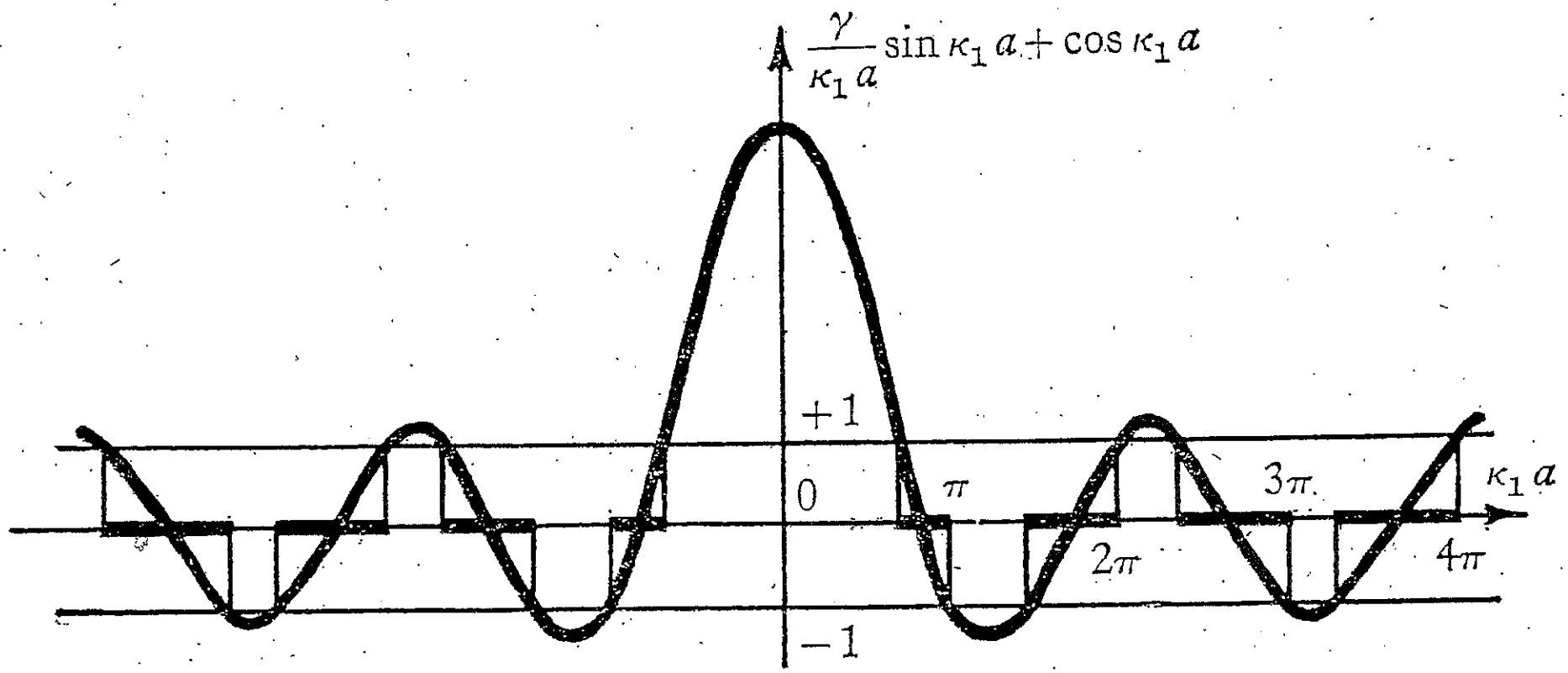
$\frac{\gamma}{\kappa_1 a}\sin\kappa_1 a+\cos\kappa_1 a$
+1
0
−1
π
2π
3π
4π
$\kappa_1 a$

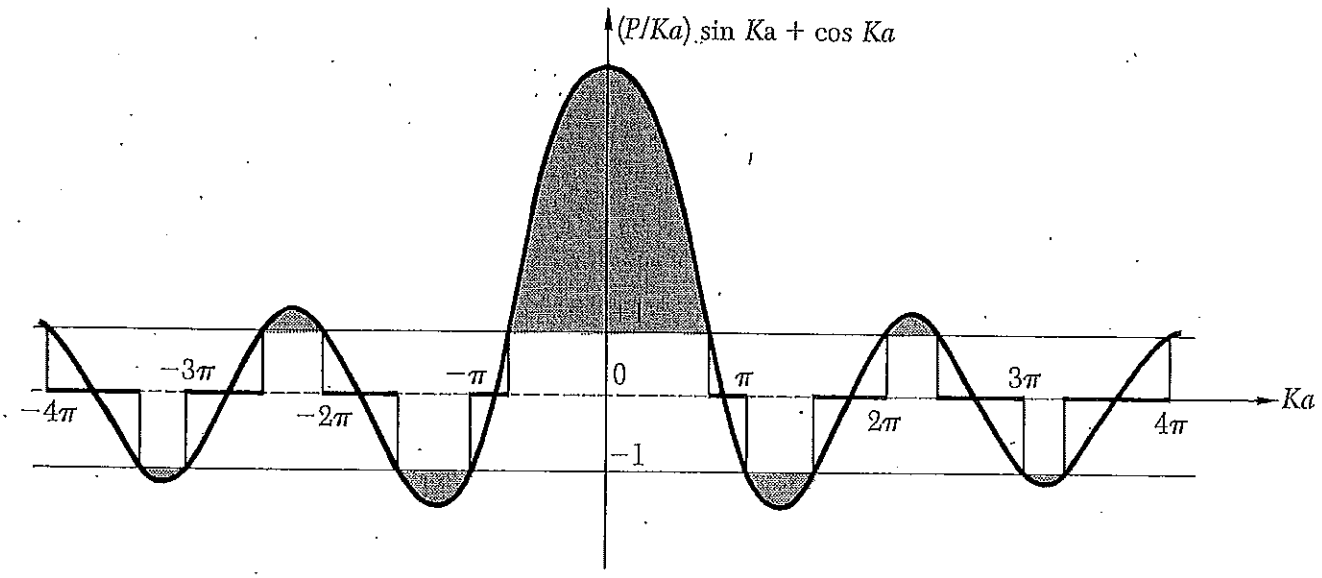

Figure 5 Plot of the function $(P/Ka)\sin Ka + \cos Ka$, for $P = 3\pi/2$. The allowed values of the energy ϵ are given by those ranges of $Ka = (2m\epsilon/\hbar^2)^{1/2}a$ for which the function lies between ± 1. For other values of the energy there are no traveling wave or Bloch-like solutions to the wave equation, so that forbidden gaps in the energy spectrum are formed.

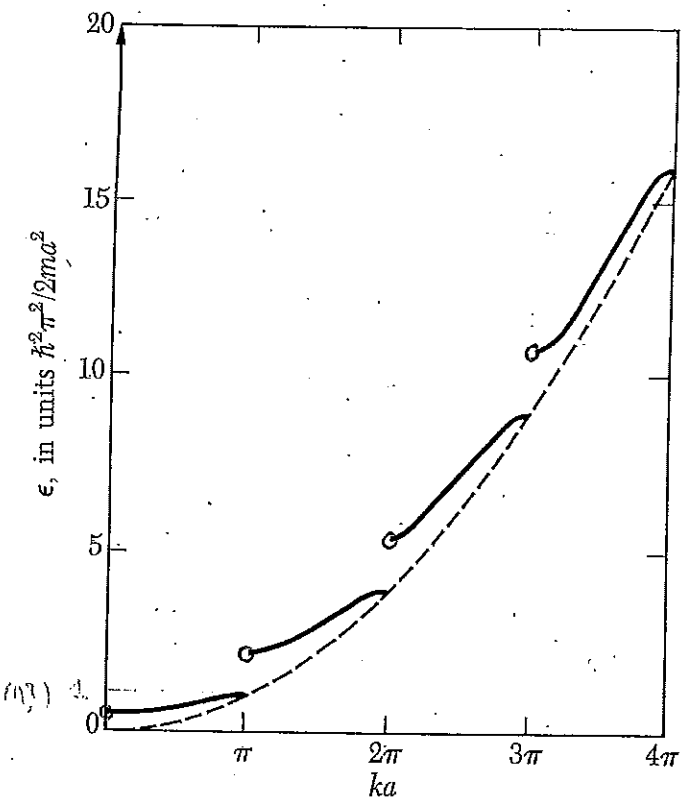

Figure 6 Plot of energy vs. wavenumber for the Kronig-Penney potential, with $P = 3\pi/2$. Notice the energy gaps at $ka = \pi, 2\pi, 3\pi \ldots$.

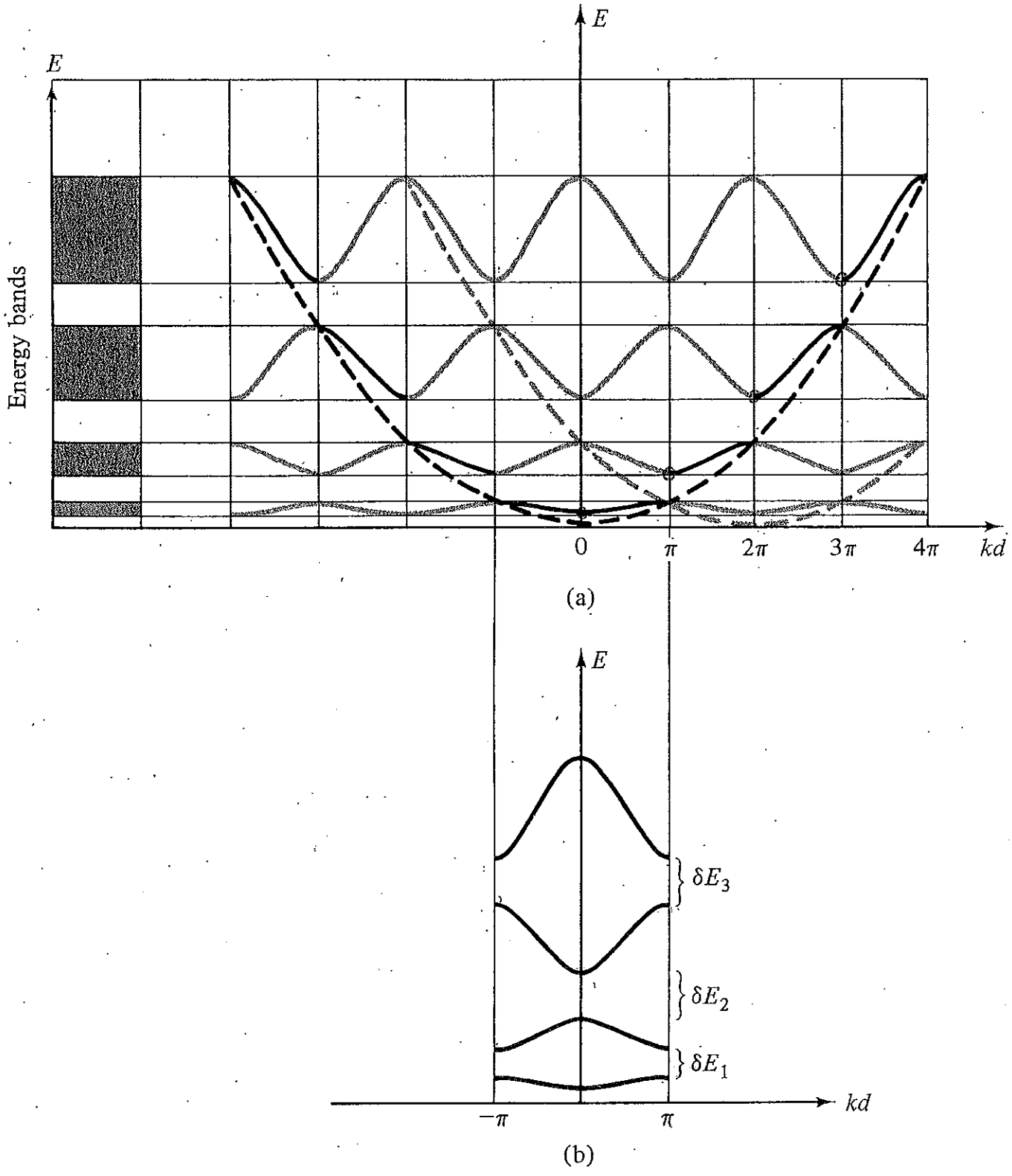

FIGURE 8.13 (a) Typical E versus k curves for the Kronig–Penney potential. The graininess of the curves stems from the fact that the k values in each band are discrete [i.e., $kd = (n/N)2\pi$, $N \gg 1$ or, equivalently, $(\Delta k)_{\text{min}} = \pi/L$]. (b) The first four bands in the reduced-zone scheme. Also shown are the first three energy gaps, δE_1, δE_2, and δE_3.

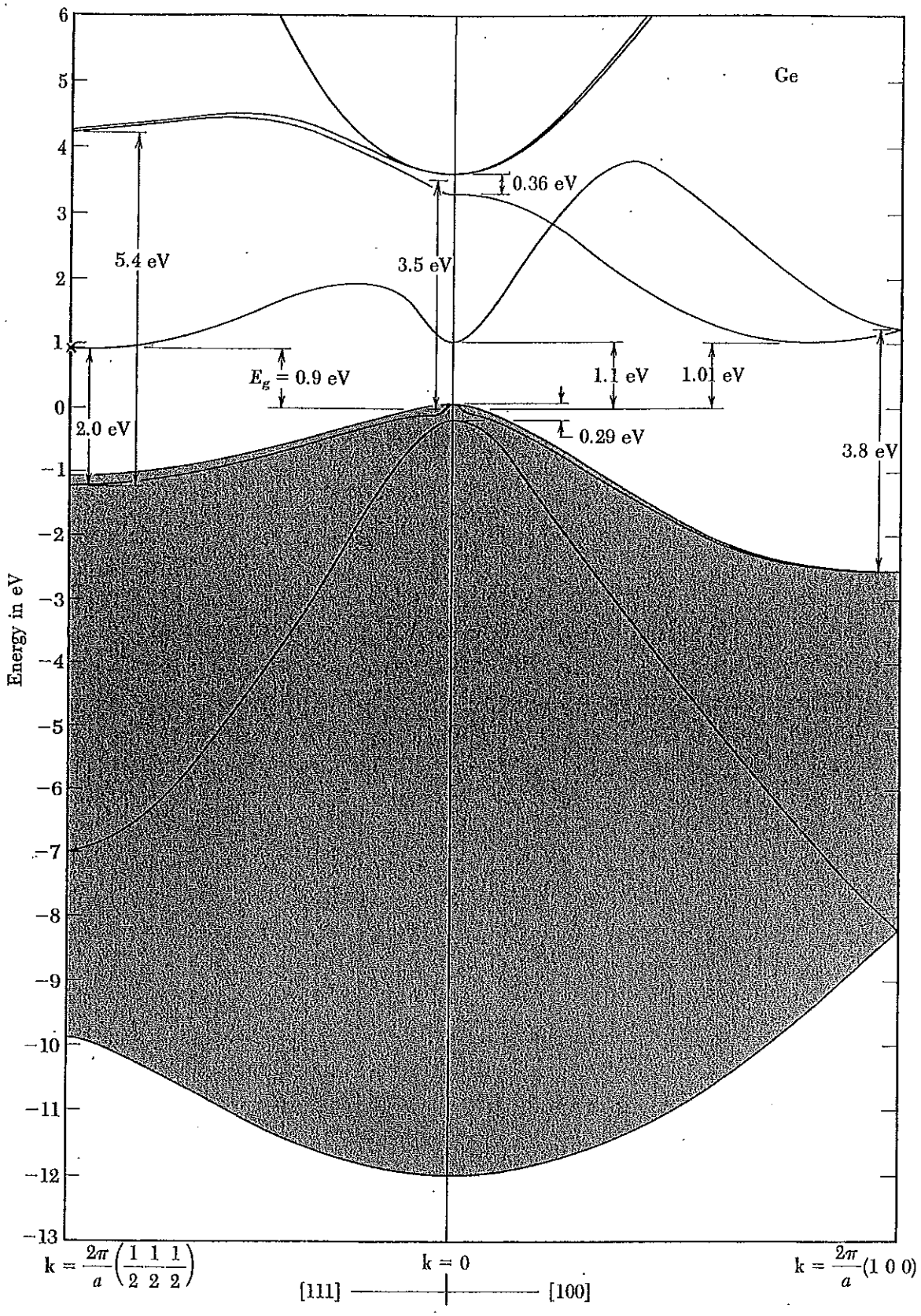

Figure 14 Calculated band structure of germanium, after C. Y. Fong. The general features are in good agreement with experiment. The four valence bands are shown in gray. The fine structure of the valence band edge is caused by spin-orbit splitting. The energy gap is indirect; the conduction band edge is at the point $(2\pi/a)(\frac{1}{2}\frac{1}{2}\frac{1}{2})$. The constant energy surfaces around this point are ellipsoidal.

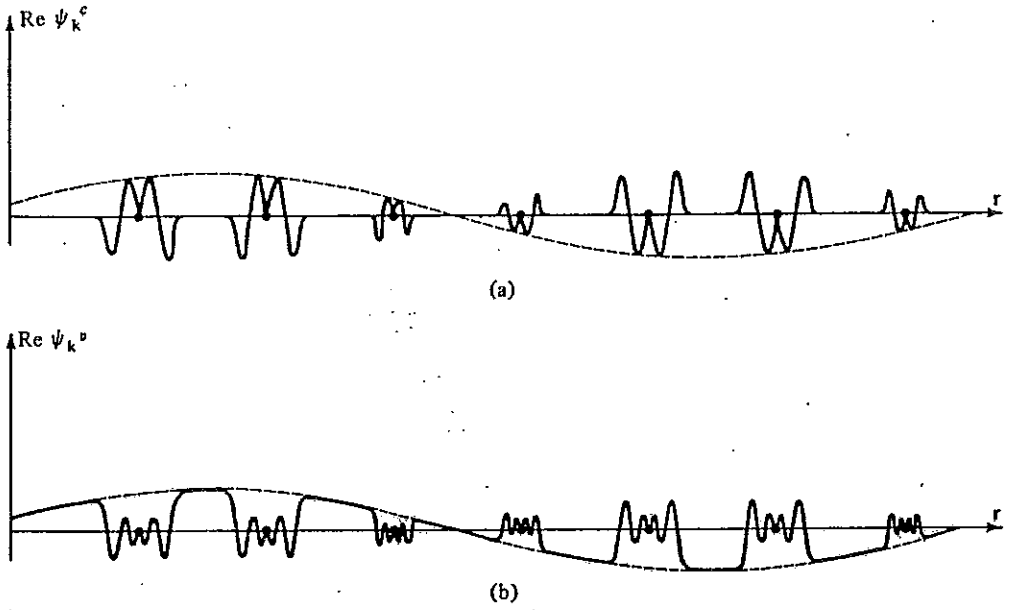

Figure 11.2
(a) Characteristic spatial dependence of a core wave function $\psi_k{}^c(\mathbf{r})$. The curve shows Re ψ against position along a line of ions. Note the characteristic atomic oscillations in the vicinity of each ion. The dashed envelope of the atomic parts is sinusoidal, with wavelength $\lambda = 2\pi/k$. Between lattice sites the wave function is negligibly small. (b) Characteristic spatial dependence of a valence wave function $\psi_k{}^v(\mathbf{r})$. The atomic oscillations are still present in the core region. The wave function need not be at all small between lattice sites, but it is likely to be slowly varying and plane-wavelike there.

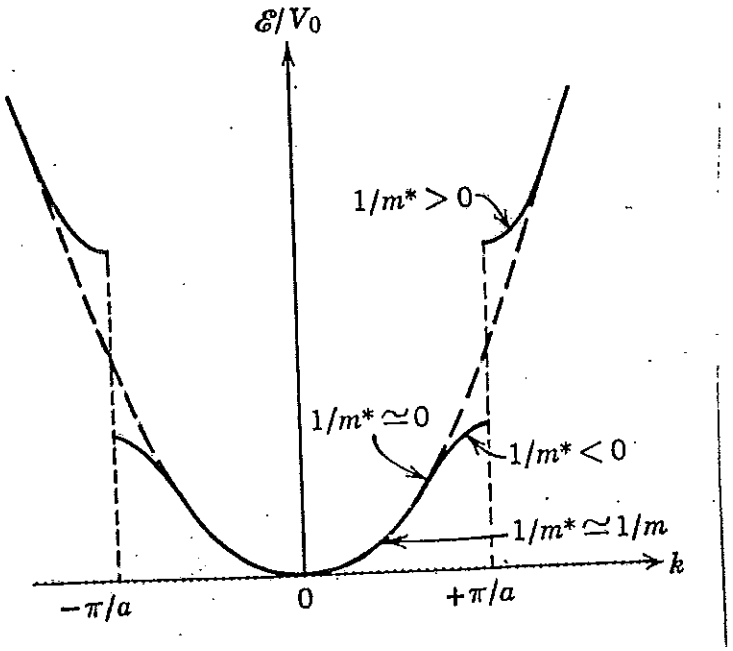

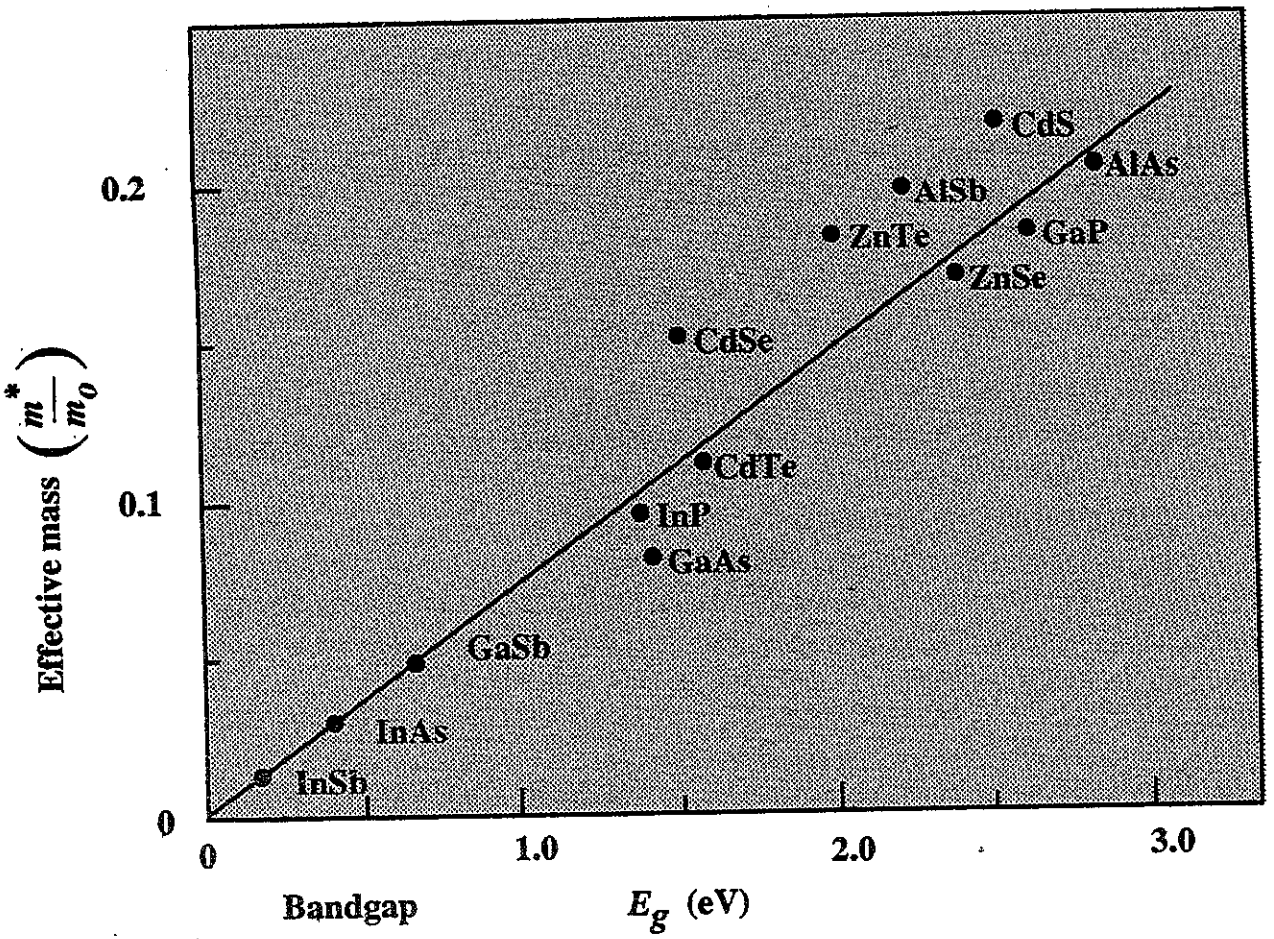

Figure 2.15: Electron effective mass $m*$ as a function of the lowest direct gap E_g for various compound semiconductors. It is interesting to note that the effective mass decreases as the bandgap decreases.

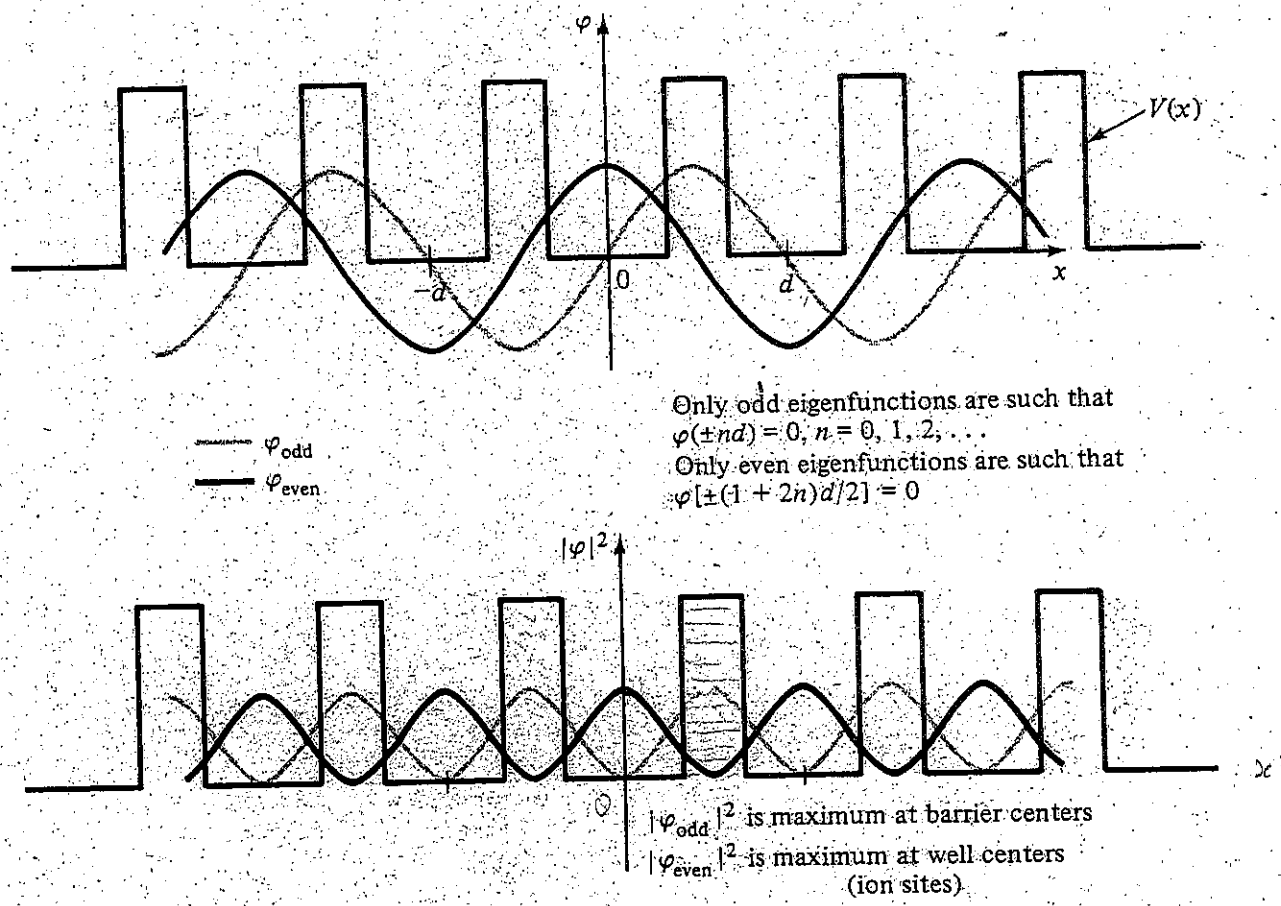

FIGURE 8.20 Typical pair of eigenfunctions for the Kronig–Penney Hamiltonian at the band edges: $kd = (2q + 1)\pi$. Periodicity of φ is $2d$.

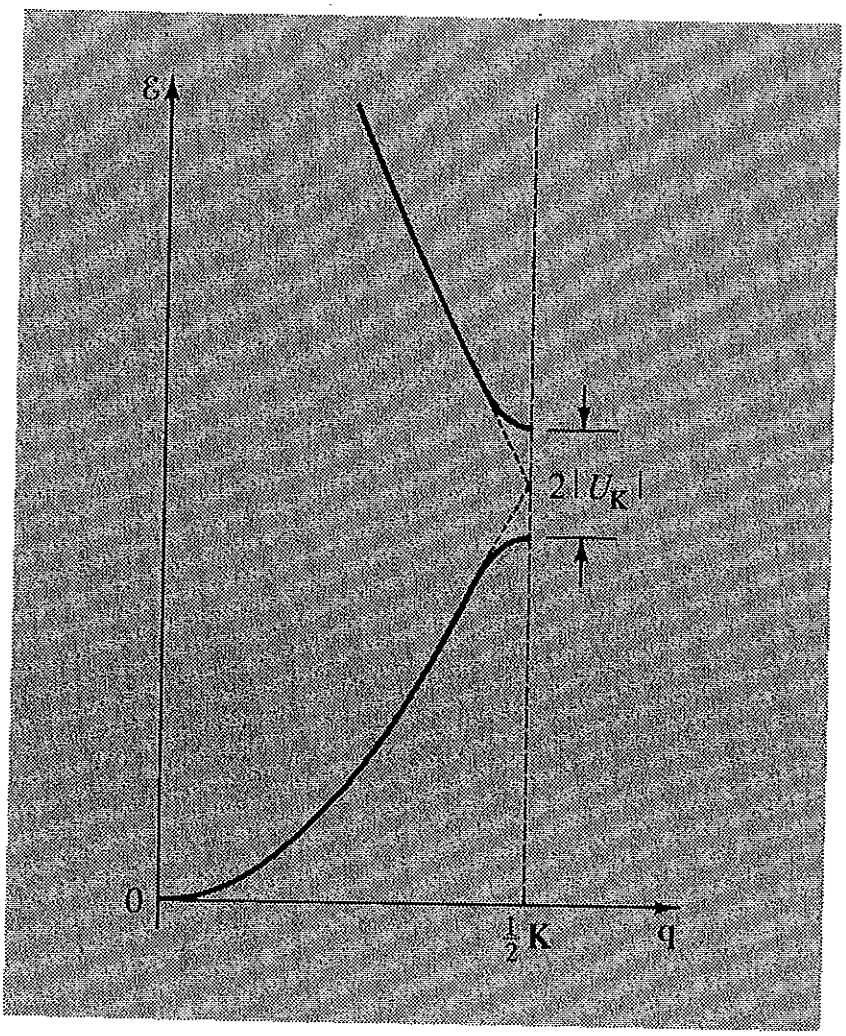
ε
2|U_K|
0
½K
q

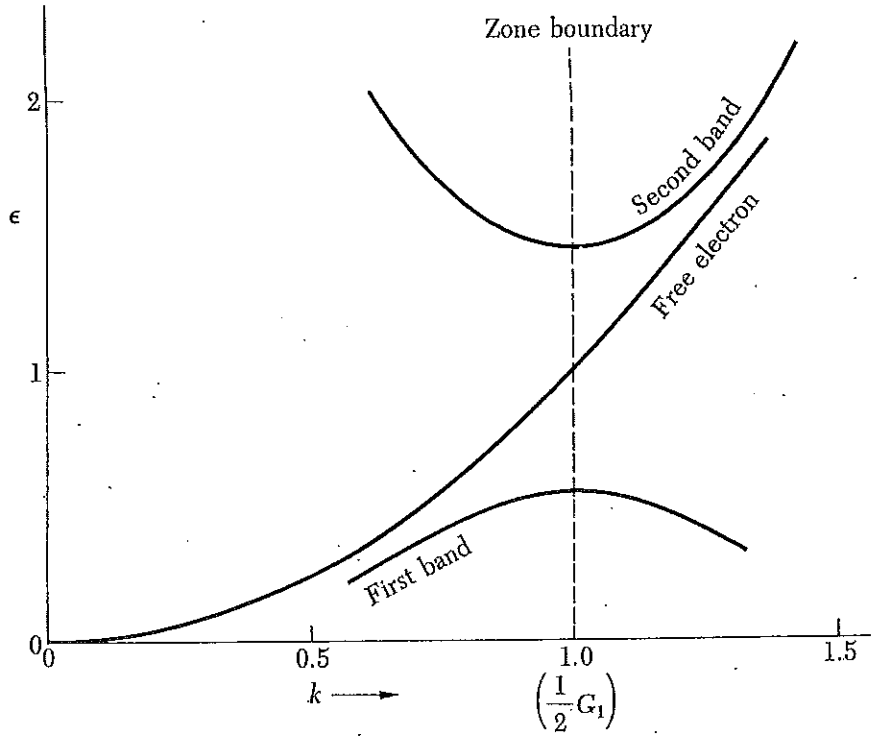

Figure 9 Solutions of (50) in the periodic zone scheme, in the region near a boundary of the first Brillouin zone. The units are such that $U = -0.45$; $G = 2$, and $\hbar^2/m = 1$. The free electron curve is drawn for comparison. The energy gap at the zone boundary is 0.90. The value of U has deliberately been chosen large for this illustration, too large for the two-term approximation to be accurate.